DELFT UNIVERSITY OF TECHNOLOGY

FACULTY OF AEROSPACE ENGINEERING

AE3211-I

SYSTEMS ENGINEERING & AEROSPACE DESIGN

Aircraft Assignment

The effects of radical propulsive solutions on the characteristics of regional aircraft

Lecturer: Dr. Fabrizio Oliviero l

March 29, 2022

Group 45

Oleksandr Krochak	5015529	Julie Paddeu	4997522
João Rodríguez	4993578	Oliver Ross	5008042
Lorenz Veithen	5075211	Niek Zandvliet	4796403

TU Delft Delft University of Technology

Contents

List of Figures

List of Tables

1 Introduction

In this report the aircraft part of the tutorial assignment for the course AE3211-I Systems Engineering and Aerospace Design will be presented. More specifically, the team was assigned with the task to perform a stability and controllability assessment of the Bombardier CRJ-1000 aircraft. Moreover, AeroSpark, a European engineering company specialized in the modification of-out-of production aircraft, started a collaboration project with Mitsubishi, to evaluate the possible benefits of re-designing the bombardier CRJ-1000, into a hybrid electric version, the CRJ-EXX. However, to finalise the conceptual design the stability and controllability of this new version also need to be investigated. First, all the key aircraft parameters and dimensions used to analyse the stability and controllability of the aircraft will be presented in chapter 2, together with the according loading diagram and scissor plot. Subsequently, in chapter 3 the hybrid electric version of the Bombardier CRJ-1000, the CRJ-EXX, will be analysed and evaluated in more detail.

Stability and Controllability Analysis of the Bombardier CRJ-1000

2

In this chapter the stability and controllability of the bombardier CRJ-1000 aircraft will be presented. Before presenting all the key parameters and dimensions used to perform the S&C analysis, the techinal drawings presenting the dimensional parameters and lay-out of the Bombardier CRJ-1000 are displayed in Figure 2.1.

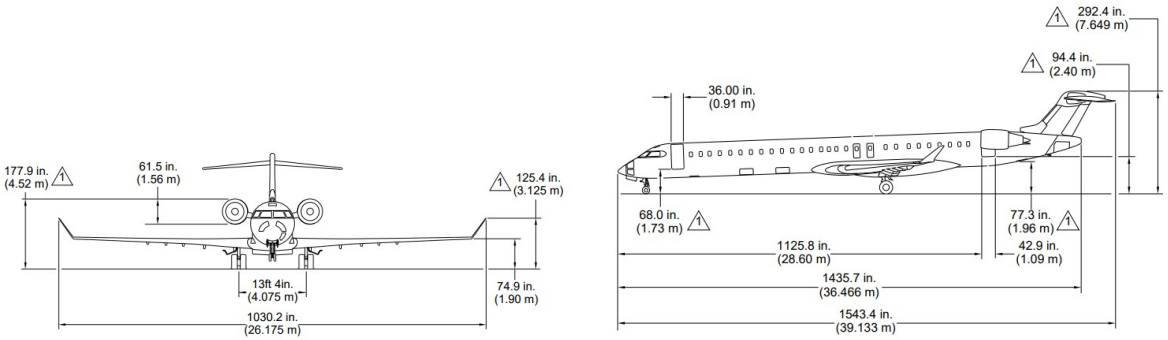

(a) Front view of the Bombardier CRJ-1000 (b) Side view of the Bombardier CRJ-1000

Figure 2.1: Technical Drawing of the Bombardier CRJ-1000 [1]

2.1 Parameters Used for Determination of Centre of Gravity Position and Loading Diagram

In this section all the parameters used to generate the loading diagram of the Bombardier CRJ-1000 will be presented. This includes the different weight contributions of the aircraft and the the centre of gravity position of the empty aircraft, the passengers, the cargo, and the fuel. The different weights of the aircraft can be found in Table 2.1. Furthermore, the centre of gravity of the empty aircraft was estimated to be at $19.4m$, or at 32% of the MAC. This was retrieved from [2] where the cg@OEW is given at 32 % of MAC.

Table 2.1: CRJ-1000 Weights

Description	Weight	Percentage of MTOW [%]
Maximum Take-Off Weight (MTOW)	91800 lb (41640 kg)	100
Operational Empty Weight (EOW)	51120 lb (23188 kg)	55.7
Maximum Payload Weight	23380 lb (11966 kg)	28.7
Fuel Weight at Maximum Payload Weight	14299 lb (6486 kg)	15.6
Passenger & Cabin Luggage Weight	20975 lb (9514 kg)	22.8
Front Cargo Hold Weight	1973 lb (895 kg)	2.2
Aft Cargo Hold Weight	3433 lb (1557 kg)	3.7

To generate the loading diagram, the required arm with respect to the nose of the aircraft is needed. For that, we assumed a specific passenger configuration of 4 seat abreast and 25 row with seat pitch of 31 inches. This is a common commercial configuration that was adopted by the group to allow for the generation of a loading diagram. On top of the 100 seats for passengers there are 4 extra seats for the crew, 2 for flight attendants and 2 for the pilots, the jump seat was assumed to always be empty. The aircraft configuration can be seen on Figure 2.2.

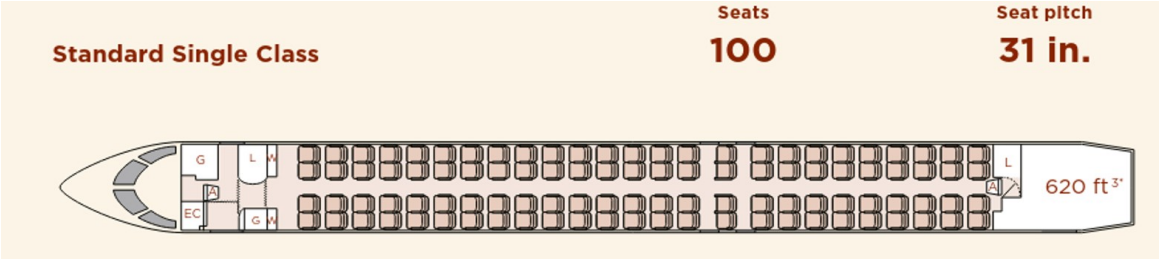

Figure 2.2: Cabin configuration for the CRJ-1000 [3]

From Figure 2.3 an approximate position of each passenger seat can be obtained by making use of the seat pitch and overwing emergency exits position, namely by making use of parameters $M = 18.49m$ and $N = 19.56m$. From there, the location of row 15 and 17 were obtained by subtracting and adding the seat pitch to the emergency door position respectively, $R_{15} = M - 0.787m$ and $R_{17} = N + 0.787m$. The x position of the remaining 23 rows were obtained by subtracting or adding a seat pitch depending on their position with respect to R_{15} and R_{17}. For the aft flight attendant the seat position was assumed to be one seat pitch behind R_{25} and for the forward one to be roughly around position $I = 4.22m$. Similarly, for the aft and forward cargo hold the same approach is taken by making use of the door length and position on the fuselage. For the forward cargo hold $C_f = \frac{K+L}{2} + \frac{door\ length}{2} = 11.845m$ and for the aft cargo hold $C_a = O + \frac{door\ length}{2} = 29.145m$.

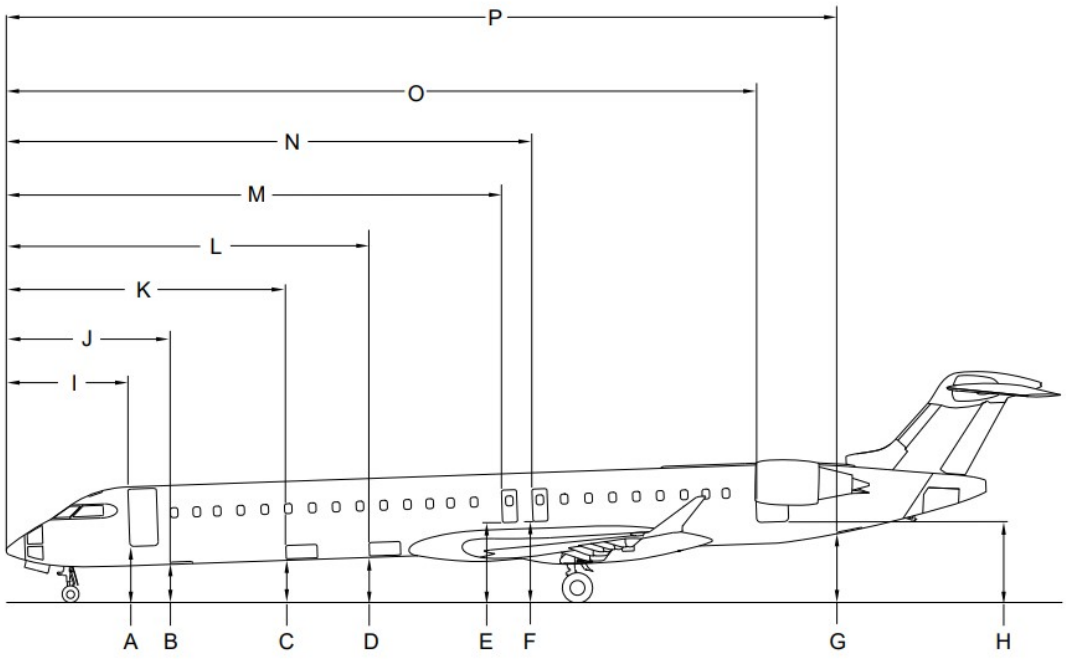

Figure 2.3: Door clearances and position for the CRJ-1000 [1]

For the position of the fuel tanks, it was assumed that the center tank would be at half the root chord $F_c = l_{fn} + \frac{c_{root}}{2} = 18.89m$ and the wing tanks would be located at half the MAC $F_w = x_{LEMAC} + \frac{MAC}{2} = 19.99m$. These aerodynamic parameters were calculated and will be explained in section 2.3.

Next, the weight of each component needed to be estimated. For the passengers, historical data and statistical data found returned a value of $m = 83.4kg$ [4] on average; a margin of 10% was added on top of that as a conservative measure yielding a total mass, including carry- on bags, of $m_{pax} = 91.74kg$. Each pilot and flight attendant was assumed to have a mass of $m_{pilot} = 95kg$ and $m_{attendant} = 75kg$.

The mass of each cargo hold was computed based on their volume by proportionally distributing the mass between both cargo holds. The aft cargo volume is $V_a = 14.41m^3$ and the forward one is $V_f = 5.26m^3$

meaning that roughly 36.5% of the cargo weight is carried by the forward compartment and the remaining 63.5% in the aft compartment. The total cargo weight was computed by subtracting the maximum payload weight with the fully loaded passenger plus crew of the aircraft $W_{c_{total}} = W_{c_{aft}} + W_{c_{forward}} = W_{P_{max}} - W_{people} = 2452kg$. Distributing this over the two cargo holds yields: $W_{c_{aft}} = 1556.96kg$ and $W_{c_{forward}} = 895.04kg$. A similar approach was taken to estimate the fuel mass. The fuel weight at maximum payload weight, given in Table 2.1, is distributed proportionally between both tanks. From [2] it was found that 69% of the fuel is carried by the wing tanks and the remaining 31% by the center tank, resulting in $Wf_w = 0.69 \cdot 6486kg = 4478.11kg$ and $Wf_c = 0.31 \cdot 6486kg = 2007.89kg$

Weight and balance sheet CRJ 1000

	Weight [kg]	arm [m]	Passenger actual	max	Total Weight [kg]	Moment [kg*m]
Dry Weight	23188	19.40	X	X	23188	449897.36
Pilots	95	1.86	0	2	0	0
Forward Flight Attendant	75	4.22	0	1	0	0
Aft FlightAttendant	75	27.43	0	1	0	0
row 1	91.74	6.68	0	4	0	0
row 2	91.74	7.47	0	4	0	0
row 3	91.74	8.25	0	4	0	0
row 4	91.74	9.04	0	4	0	0
row 5	91.74	9.83	0	4	0	0
row 6	91.74	10.62	0	4	0	0
row 7	91.74	11.40	0	4	0	0
row 8	91.74	12.19	0	4	0	0
row 9	91.74	12.98	0	4	0	0
row 10	91.74	13.77	0	4	0	0
row 11	91.74	14.55	0	4	0	0
row 12	91.74	15.34	0	4	0	0
row 13	91.74	16.13	0	4	0	0
row 14	91.74	16.92	0	4	0	0
row 15	91.74	17.70	0	4	0	0
row 16	91.74	19.28	0	4	0	0
row 17	91.74	20.35	0	4	0	0
row 18	91.74	21.13	0	4	0	0
row 19	91.74	21.92	0	4	0	0
row 20	91.74	22.71	0	4	0	0
row 21	91.74	23.50	0	4	0	0
row 22	91.74	24.28	0	4	0	0
row 23	91.74	25.07	0	4	0	0
row 24	91.74	25.86	0	4	0	0
row 25	91.74	26.65	0	4	0	0
Forward Cargocompartment	895.04	11.85	0	1	0	0
Aft Cargocompartment	1556.96	29.15	0	1	0	0
Zero Fuel Weight (MZFW)	**35154**			X	23188	449897.36
			Fuel			
Fuel Wing tanks (left+Right)	4478.11	19.99	0	1	0.00	0.00
Fuel Center tank	2007.89	18.89	0	1	0.00	0.00
FW@PL_max	**6486.00**					
				xcg	Takeoff weight	Moments
MTOW	**41640**			19.40	23188	449897.36

Figure 2.4: Overview of arms and masses shown for empty aircraft

An overview of the parameters presented in this section can be seen above. Figure 2.4 shows the weight and balance sheet generated by the group for the empty aircraft. Note the cg@OEW at the bottom of the sheet in brown. This tool will be used to generate the full loading diagram in section section 2.4

2.2 Aerodynamic Parameters

For the aerodynamic characteristics of the aircraft, an airfoil of NACA 23018 will be used, since it is close in aerodynamic performance to airfoils used in commercial aircraft [5]. For this airfoil, taking Reynold's number Re of $1'000'000$ for the cruise condition and $Re = 50'000$ for take-off and landing conditions, the relevant parameters were found [6]:

Re	50'000	1'000'000
C_{l_0}	0.5	0.125
C_{m_0}	-0.06	-0.003
$\Delta C_{L_{fl}}$	0.7	
$\Delta C_{M_{fl}}$	-0.2	

Table 2.2: Aerodynamic Parameters of CRJ-1000.

The aircraft is assumed to have plain flaps, based on its external geometry. Aircraft with such configuration usually have C_{Lmax} of 1.5 [7]. Additionally, at low Reynold's numbers NACA 23018 airfoil has $C_{Lmax} = 0.8$, so then the additional lift coefficient due to flaps will be $\Delta C_L = 0.7$, which was assumed to be constant regardless of the angle of attack. This allows us to take $C_{L_{\alpha=0}}$ to also be 0.7 in order to find the moment contribution due to the flap deflection $\Delta C_M = -0.2$ from the experimental data from Obert [8].

2.3 Geometrical Parameters

Geometrical parameters of CRJ-1000 were either found on the manufacturing website [3], airport manual [1] or derived from the three-view drawings with the help of MATLAB in Figure B.1b. Mean aerodynamic chord for a kinked wing was taken as a weighted average of two parts of the wing with their surface area as reference:

$$\bar{c} = \frac{S_1 \cdot \bar{c_1} + S_2 \cdot \bar{c_2}}{S_1 + S_2} \tag{2.1}$$

The parameters for the main wing and empennage, as well as the fuselage, are presented in the following table:

Table 2.3: Geometric Parameters of the Bombardier CRJ-1000

Fuselage			Main wing			Horizontal stabilizer		
$l_{a/c}$	39.13	[m]	S	77.4	$[m^2]$	S_h	15.91	$[m^2]$
b_f	2.7	[m]	b (w.o. winglets)	23.395	[m]	b_h	8.54	[m]
$h_{a/c}$	7.47	[m]	A	8.85	[-]	A_h	4.59	[-]
l_n	14.15	[m]	λ	0.265	[-]	λ_h	0.465	[-]
l_h	17.93	[m]	Λ	29.6	[deg]	Λ_h	32.4	[deg]
l_{fn}	16.33	[m]	$\Lambda_{c/4}$	25.6	[deg]	$\Lambda_{c/4_h}$	29.7	[deg]
l_f	36.47	[m]	$\Lambda_{c/2}$	21.2	[deg]	$\Lambda_{c/4_h}$	27.1	[deg]
$X_{LE,MAC}$	18.35	[m]	$\bar{c}$ (MAC)	3.29	[m]	$\bar{c}$ (MAC)	1.94	[m]

2.4 Generation of the Loading Diagram

In this section the loading diagram for the CRJ-1000 will be shown based on the presented data on section 2.1. An overview of the main x_{cg} positions and aircraft states can be seen on Table 2.4. The following order was followed when constructing the loading diagram

- Loading the crew
- Loading the cargo holds
- Loading window seat passengers
- Loading aisle seat passengers
- Loading the fuel

The final result of the loading diagram can be seen on Figure 2.5. Some key weight parameters are also included along the way for future comparison reason to the modified configuration, the scale is also chosen to allow for the plot of the modified CRJ later. Information on the main center of gravity locations can be seen on Table 2.4.

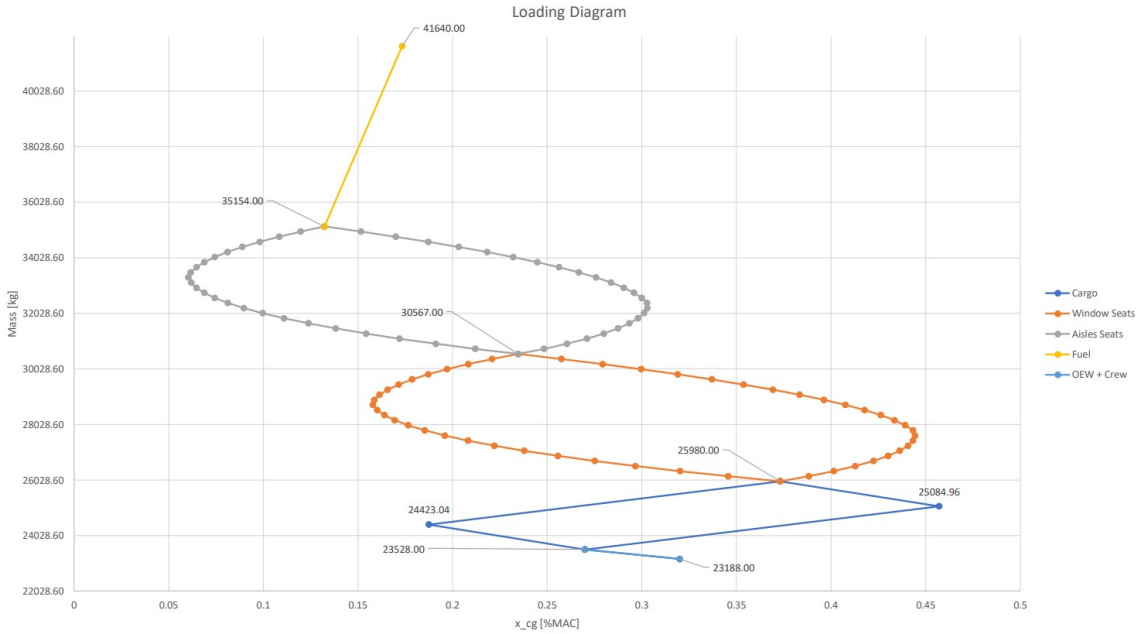

Figure 2.5: Loading Diagram for the CRJ-1000

Table 2.4: Overview main x_{cg} positions

	$x_{cg}[m]$	$x_{cg}[\%MAC]$	Mass at state [kg]	Configuration
x_{cg} @OEW	19.402	0.3200	23188.00	Empty Aircraft
x_{cg} @OEW + crew	19.238	0.2699	23528.00	Empty Aircraft plus crew
Most aft x_{cg}	19.853	0.4571	25084.96	Loading back cargo before front cargo
Most aft x_{cg} + 2% margin	19.883	0.4662	-	-
Most forward x_{cg}	18.549	0.0604	33319.20	Loading aisle seat from front to back at row 15
Most forward x_{cg} - 2% margin	18.545	0.0592	-	-
x_{cg} range with 2% margin	**1.337**	**0.4070**	-	-
x_{cg} position cargo and tanks				
x_{cg} forward cargo	11.845	-1.9800	-	-
x_{cg} aft cargo	29.145	3.2852	-	-
x_{cg} center tank	18.885	0.1626	-	-
x_{cg} wing tanks	19.994	0.5000	-	-

2.5 Generation Scissor Plot

In this section the different steps taken in order to generate the scissor plot will be provided. First, the generation of the stability graph will be discussed in more detail, in subsection 2.5.1, which is followed on a discussion on the generation of the controllability graph in subsection 2.5.2. Finally, the scissor plot will be presented in subsection 2.5.3.

2.5.1 Stability

The stability of the aircraft needs to be determined for cruise conditions, since this is the critical condition during flight for the stability of the aircraft. The maximum Mach number at cruise of the bombardier CRJ-1000 was found to be of Mach 0.82, which leads to a β (compressibility factor $\sqrt{1-M^2}$) of 0.57. Furthermore,

the stability margin was set to 5%. Now, looking at Equation 2.2, which describes the stability graph, the parameters that had to be determined to generate the stability graph are $\overline{x}_{ac}$, $C_{L\alpha_h}$, $C_{L\alpha_{A-h}}$, $\frac{d\epsilon}{d\alpha}$, and $(\frac{V_h}{V})^2$.

$$\frac{S_h}{S} = \overline{x}_{cg} \cdot \frac{1}{\frac{C_{L\alpha_h}}{C_{L\alpha_{A-h}}}(1-\frac{d\epsilon}{d\alpha})\frac{l_h}{\overline{c}}(\frac{V_h}{V})^2} - \frac{\overline{x}_{ac} - S.M.}{\frac{C_{L\alpha_h}}{C_{L\alpha_{A-h}}}(1-\frac{d\epsilon}{d\alpha})\frac{l_h}{\overline{c}}(\frac{V_h}{V})^2} \tag{2.2}$$

The first parameter that will be discussed is the aerodynamic center of the aircraft. This parameter can be approximated by Equation 2.3. First $(\overline{x}_{ac})_w$ was estimated using an estimation method presented by Torenbeek. Important here is that the graph for $\beta A = 4$ was used and not the graph for $\beta A = 6$, since the Bombardier CRJ-1000 has an βA of 5 and we over-estimate for the most critical condition. Using Figure 2.6, this leads to a $(\overline{x}_{ac})_w$ of 0.36. Now $(\overline{x}_{ac})_{f1}$ and $(\overline{x}_{ac})_{f2}$ were calculated using Equation 2.4 and Equation 2.5 respectively. Finally, $(\overline{x}_{ac})_n$ was estimated using Equation 2.6, with $k_n = -2.5$, since the jet engines are mounted to the sides of the rear fuselage.

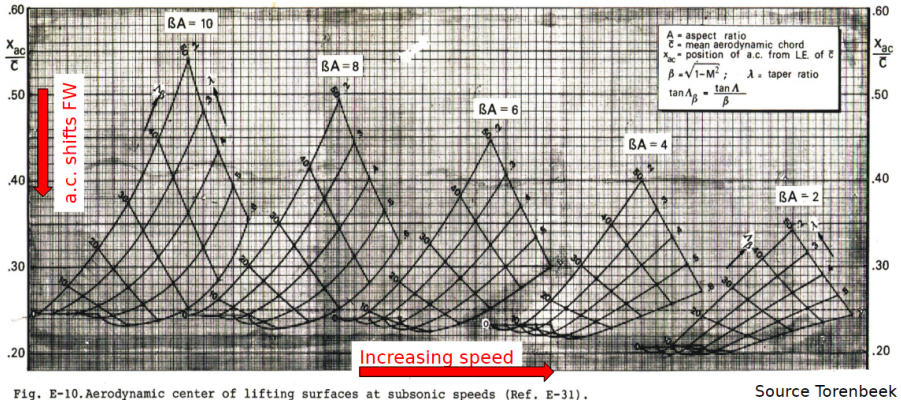

Figure 2.6: Graph for the x_{ac_w} *Determination*

$$x_{ac} = (\overline{x}_{ac})_w + (\overline{x}_{ac})_{f1} + (\overline{x}_{ac})_{f2} + (\overline{x}_{ac})_n \tag{2.3}$$

$$(\overline{x}_{ac})_{f1} = -\frac{1.8}{C_{L\alpha_{A-h}}}\frac{b_f h_f l_{fn}}{S\overline{c}} \tag{2.4}$$

$$(\overline{x}_{ac})_{f2} = \frac{0.273}{1+\lambda}\frac{b_f c_g (b-b_f)}{\overline{c}^2(b+2.15b_f)} tan\Lambda_{1/4} \tag{2.5}$$

$$(\overline{x}_{ac})_n = \sum k_n \frac{b_n^2 l_n}{S\overline{c}C_{L\alpha_{A-h}}} \tag{2.6}$$

Now, the equations used to calculate $C_{L\alpha_h}$ and $C_{L\alpha_{A-h}}$ are Equation 2.7 and Equation 2.8 respectively. In the latter equation $C_{L\alpha_w}$ is calculated using the DATCOM method.

$$C_{L\alpha_h} = \frac{2\pi A_h}{2+\sqrt{4+(\frac{A_h\beta}{\eta})^2 \cdot (1+(\frac{tan\Lambda_{0.5}}{\beta})^2)}} \tag{2.7}$$

$$C_{L\alpha_{A-h}} = C_{L\alpha_w} \cdot (1+2.15\frac{b_f}{b})\frac{S_{net}}{S} + \frac{\pi}{2}\frac{b_f^2}{S} \tag{2.8}$$

Finally, the downwash $\frac{d\epsilon}{d\alpha}$ was assumed to be zero since a the bombardier CRJ-1000 has a T-tail, and $(\frac{V_h}{V})^2$ was determined to be equal to 1 [8].

Now a summary of all the stability parameters determined is shown in Table 2.5.

Stability parameters		
$\overline{x}_{ac_w}$	0.36	[-]
$\overline{x}_{ac_{f1}}$	-0.128	[-]
$\overline{x}_{ac_{f2}}$	0.056	[-]
$\overline{x}_{ac_n}$	-0.1023	[-]
$\overline{x}_{ac}$	0.1857	[-]
$C_{L\alpha_h}$	4.64	[1/rad]
$C_{L\alpha_w}$	6.36	[1/rad]
$C_{L\alpha_{A-h}}$	6.53	[1/rad]
$\frac{d\epsilon}{d\alpha}$	0	[-]
$(\frac{V_h}{V})^2$	1	[-]

Table 2.5: Stability Parameters for the Bombardier CRJ-1000

2.5.2 Controllability

The next step was generating the controllability graph. In order to do this some extra parameters had to be determined. Looking at Equation 2.9 the parameters that needed to be found were C_{L_h}, $C_{L_{A-h}}$, and $C_{m_{ac}}$.

$$\frac{S_h}{S} = \frac{1}{\frac{C_{L_h}}{C_{L_{A-h}}}\frac{l_h}{\overline{c}}(\frac{V_h}{V})^2}\overline{x}_{cg} + \frac{\frac{C_{m_{ac}}}{C_{L_{A-h}}} - \overline{x}_{ac}}{\frac{C_{L_h}}{C_{L_{A-h}}}\frac{l_h}{\overline{c}}(\frac{V_h}{V})^2} \tag{2.9}$$

First, C_{L_h} was set to -0.8, since the Bombardier CRJ-1000 has an adjustable tail [8]. Furthermore, $C_{L_{A-h}}$, was set equal to the maximum lift coefficient 1.5 as it was assumed that the lift coefficient of the aircraft at landing without the tail will be close the lift coefficient of the wing of the aircraft. Finally, $C_{m_{ac}}$ was determined using Equation 2.10.

$$C_{m_{ac}} = C_{m_{ac_w}} + \Delta_f C_{m_{ac}} + \Delta_{fus} C_{m_{ac}} + \Delta_{nac} C_{m_{ac}} \tag{2.10}$$

with $\Delta_{nac}C_{m_{ac}}$ assumed to be negligible, $\Delta_{fus}C_{m_{ac}}$ determined using wind tunnel test data from Obert [8] with $\Delta C_{L_{fl}} = 0.7$, $C_{m_{ac_w}}$ determined using:

$$C_{m_{ac_w}} = C_{m_{0airfoil}}(Acos^2\Lambda/(A + 2cos\Lambda))$$

and $\Delta_{fus}C_{m_{ac}}$ determined using:

$$\Delta_{fus}C_{m_{ac}} = -1.8(1 - \frac{2.5b_f}{l_f})\frac{\pi b_f h_f l_f}{4S\overline{c}}\frac{C_{L_0}}{C_{L\alpha_{A-h}}}$$

Furthermore, important to notice is that the controllability graph is determined for take-off and landing conditions, since these conditions are critical. The approach speed was found to be at a Mach of 0.33. This change in aircraft speed accordingly lead to a change in the aerodynamic centre of the aircraft, more specifically x_{ac} was found to be equal 0.11. It should be noted that this gives a larger design space in terms of the size of the horizontal tail since the controllability graph shifts to the left, when a Mach of 0.33 is used.

Finally, Table 2.6 provides an overview of the parameters used to determine the controllability graph.

Controllability parameters		
C_{L_h}	-0.8	[-]
$C_{m_{ac_w}}$	-0.00189	[-]
$\Delta_f C_{m_{ac}}$	-0.2	[-]
$\Delta_{fus} C_{m_{ac}}$	-0.0235	[-]
$\Delta_{nac} C_{m_{ac}}$	0	[-]
$C_{m_{ac}}$	-0.225	[-]
$C_{L_{A-h}}$	1.5	[-]
x_{ac}	0.11	[-]

Table 2.6: Controllability Parameters for the Bombardier CRJ-1000

2.5.3 Scissor Plot Bombardier CRJ-1000

Now, that all the parameters needed to generate the scissor plot are determined, the result can be seen in Figure 2.7. More specifically, this scissor plot contains the stability graph, the controllability graph, and the x_{cg} range of the Bombardier CRJ-1000.

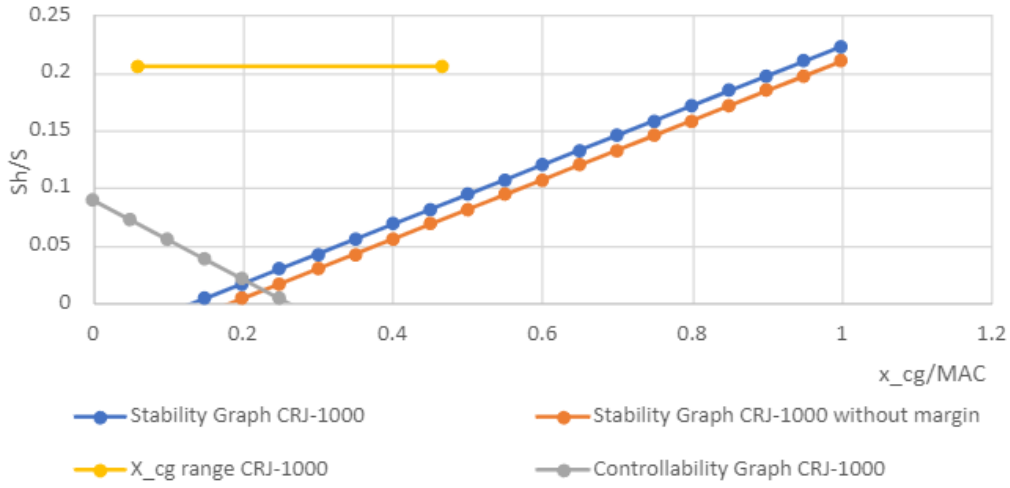

Figure 2.7: Scissor Plot for the Bombardier CRJ-1000

Evaluation of the Design Modifications 3

In this chapter the design of the hybrid electric version of the Bombardier CRJ-1000, the CRJ-EXX, will be evaluated. First, in section 3.1 the executed modifications will be presented. Subsequently, the new weight of the CRJ-EXX used to generate the loading diagram will be presented in section 3.2. This will be followed by section 3.3 in which the centre of gravity calculations for the CRJ-EXX will be presented, together with the corresponding loading diagram. Furthermore, the modified scissor plot according to the design changes will be presented in section 3.4. Moreover, in section 3.5 the questions of the customers will be presented. Finally, in section 3.6 those questions will be answered and the new design will be evaluated.

3.1 The Bombardier CRJ-EXX

As mentioned earlier, the Bombardier CRJ-EXX, is a new hybrid electric version of the Bombardier CRJ-1000. The modifications that come with this will be listed below.

- A new lightweight interior
- A new glass cockpit
- A new serial hybrid electric propulsion system

However, these modifications will lead to some important changes in the weight and design of the Bombardier CRJ-1000, which will lead to a change in the loading diagram and the stability and controllability graphs. Therefore, this new design needs to be evaluated carefully. The modifications that come with this new design are the following:

- The OEW of the CRJ-EXX will be 5% lower than the old CRJ-1000.
- The centre of gravity at operational empty weight will shift forward by $50cm$ with respect to the old position.
- The electric part of the powertrain is powered by two battery packs. The battery total weight is 3000 kg and the first pack (that accounts for a total volume of 934 liters and a weights of 1350 kg) is located in the most forward part of the forward cargo hold. The second battery pack (1650 kg, and a volume of 1142 liters) is instead located in the aft cargo compartment, in the most aft area.
- The last two rows of passengers are removed.
- A new winglet system increases the wing effective aspect ratio with 20%.
- The maximum lift coefficient of the aircraft-less-tail is increased by 20% with respect to the CRJ-1000 version due to an improvement of the high lift devices.
- The height of the landing gears is increased by $30cm$.

3.2 Calculation of Modified Weights for the CRJ-EXX

In this section the different weights of the aircraft can be found in Table 3.1. Furthermore, the centre of gravity of the empty aircraft was given to be 50cm in front of the previous configuration at a position of $18.9m$ from the nose, or at 16.8% of the MAC. This however is shifted further aft due to the addition of batteries on the cargo holds. The empty aircraft configuration is presented on the weight and balance sheet, shown on Figure 3.1. The masses and moment arms are also shown. Note the new x_{cg} @OEW + batteries at 19.07 or 0.22% of the MAC.

Table 3.1: CRJ-EXXX Weights

Description	Weight	Percentage of MTOW
Maximum Take-Off Weight (MTOW)	91800 lb (41640 kg)	100
Operational Empty Weight (EOW)	48565 lb (22029 kg)	52.9
Maximum Payload Weight	26380 lb (11966 kg)	28.7
Fuel Weight at Maximum Payload Weight	10241 lb (4645 kg)	11.2
Passenger & Cabin Luggage Weight	19357 lb (8780 kg)	21.1
Front Cargo Hold Weight	2290 lb (1039 kg)	2.5
Aft Cargo Hold Weight	4734 lb (2147 kg)	5.2
Forward Battery	2976 lb (1350 kg)	3.2
Aft Battery	3638 lb (1650 kg)	4.0

Weight and balance sheet CRJ EXX

			Passenger			
	Weight [kg]	arm [m]	actual	max	**Total Weight [kg]**	**Moment [kg*m]**
Old Dry Weight	23188	19.40				
Dry Weight	22028.6	18.90	X	X	22028.60	416388.19
Pilots	95	1.8578	2	2	190.00	352.98
Forward Flight Attendant	75	4.22	1	1	75.00	316.50
Aft FlightAttendant	75	27.434	1	1	75.00	2057.55
row 1	91.74	6.679	0	4	0.00	0.00
row 2	91.74	7.47	0	4	0.00	0.00
row 3	91.74	8.25	0	4	0.00	0.00
row 4	91.74	9.04	0	4	0.00	0.00
row 5	91.74	9.83	0	4	0.00	0.00
row 6	91.74	10.62	0	4	0.00	0.00
row 7	91.74	11.40	0	4	0.00	0.00
row 8	91.74	12.19	0	4	0.00	0.00
row 9	91.74	12.98	0	4	0.00	0.00
row 10	91.74	13.77	0	4	0.00	0.00
row 11	91.74	14.55	0	4	0.00	0.00
row 12	91.74	15.34	0	4	0.00	0.00
row 13	91.74	16.13	0	4	0.00	0.00
row 14	91.74	16.92	0	4	0.00	0.00
row 15	91.74	17.70	0	4	0.00	0.00
row 16	91.74	19.28	0	4	0.00	0.00
row 17	91.74	20.35	0	4	0.00	0.00
row 18	91.74	21.13	0	4	0.00	0.00
row 19	91.74	21.92	0	4	0.00	0.00
row 20	91.74	22.71	0	4	0.00	0.00
row 21	91.74	23.50	0	4	0.00	0.00
row 22	91.74	24.28	0	4	0.00	0.00
row 23	91.74	25.07	0	4	0.00	0.00
Forward Cargocompartment	1038.76	11.845	0	1	0.00	0.00
Aft Cargocompartment	2147.16	29.145	0	1	0.00	0.00
Forward Battery	1350	9.89	X	1	1350	13351.50
Aft Battery	1650	31.145	X	1	1650	51389.25
Zero Fuel Weight (MZFW)	**35154**			X	25368.60	483855.97
			Fuel			
Fuel Wing tanks (left+Right)	3207.31	19.99	0	1	0.00	0.00
Fuel Center tank	1438.09	18.89	0	1	0.00	0.00
FW@PL_max	**4645.40**					
				xcg	Takeoff weight	Moments
MTOW	**41640**			19.07	25368.60	483855.97

Figure 3.1: Overview of arms and masses shown for empty aircraft after modification

3.3 Calculation of the Modified Centre of Gravity for the CRJ-EXX

In this section the loading diagram for the CRJ-EXX and both loading diagrams, before and after modification, will be displayed together in the same plot. This is shown in Figure 3.2 and Figure 3.3, respectively. An overview of the main x_{cg} positions and aircraft states can be seen on Table 3.2. Some key weight parameters

are also included in the plots to allow for an easy comparison. The following loading order followed to construct the diagrams is the same as the one described in section 2.4.

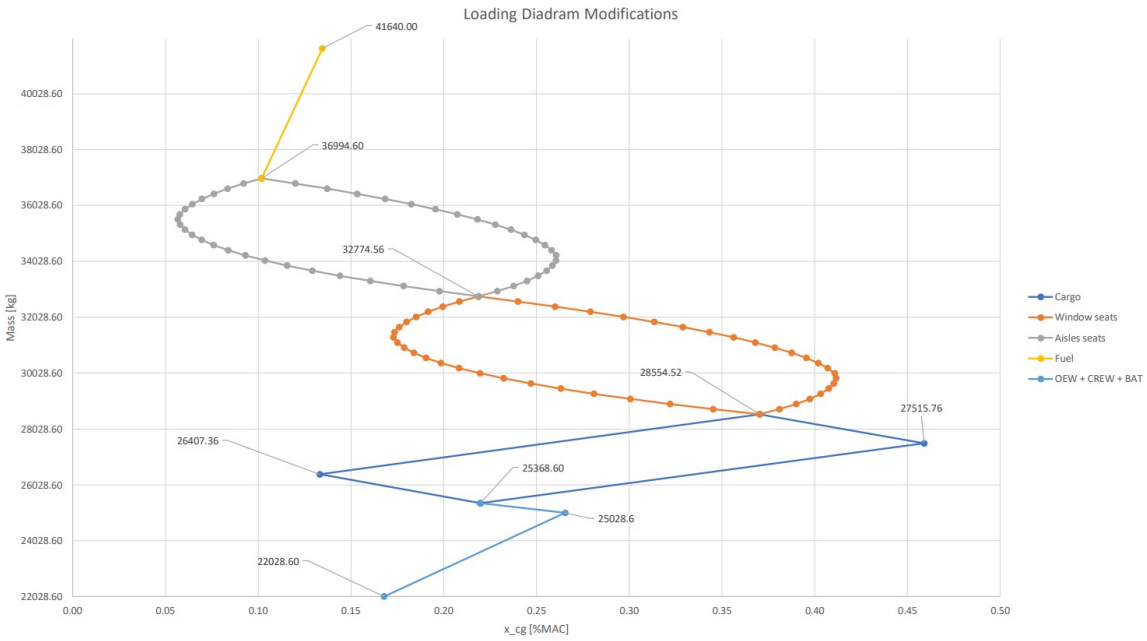

Figure 3.2: Loading Diagram for the modified CRJ-1000

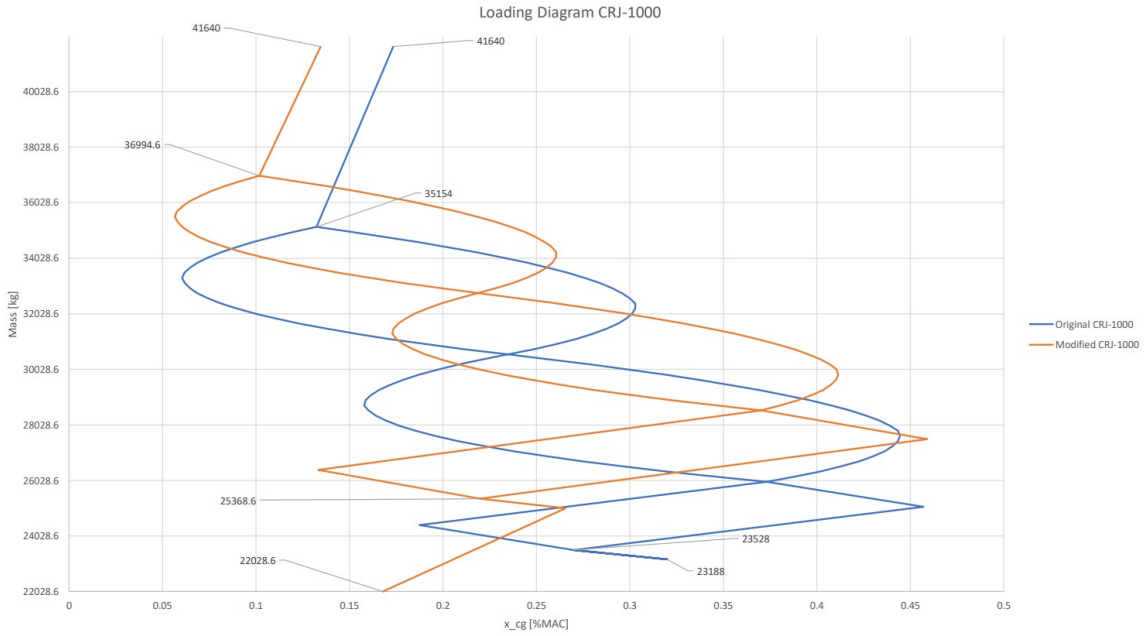

Figure 3.3: Loading Diagram comparison

The final result of the loading diagram can be seen on Figure 3.2. From Figure 3.3 it can be clearly seen the reduction of fuel carried on board due to the modification, depicted by the considerably shorter line on top of the diagram. Note as well the much higher operative weight (OEW + crew + batteries) starting at $25368.60kg$ compared to the previous CRJ-1000 configuration of $23528.00kg$. This leads to the following drawback, you either carry the same payload capacity but at a shorter range, due to the decrease amount of fuel, or alternatively, you carry less payload for the same range by decreasing payload capacity and increasing the fuel quantity. The total x_{cg} shift also slightly increases and its value can be found, along several other important x_{cg} locations, on Table 3.2

Table 3.2: Overview main x_{cg} positions after modification

	$x_{cg}[m]$	$x_{cg}[\%MAC]$	Mass at state [kg]	Configuration
x_{cg} @OEW	18.902	0.1678	22028.60	Lighet Empty Aircraft
x_{cg} @OEW plus batteries	19.223	0.2655	25028.60	Lighet Empty Aircraft plus batteries
x_{cg} @OEW plus batteries and crew	19.073	0.2198	25368.60	Lighet Empty Aircraft plus batteries and crew
Most aft x_{cg}	19.859	0.4590	27515.76	Loading back cargo before front cargo
Most aft x_{cg} + 2% margin	19.889	0.4682	-	-
Most forward x_{cg}	18.537	0.0566	35526.76	Loading aisle seat from front to back at row 15
Most forward x_{cg} - 2% margin	18.533	0.0554	-	-
x_{cg} range with 2% margin	**1.356**	**0.4128**	-	-
x_{cg} position of batteries				
x_{cg} of forward battery	9.890	-2.5750	-	-
x_{cg} of aft battery	20.533	0.6641	-	-

3.4 Modified Scissor Plot for the CRJ-EXX

In this section the scissor plot for the modified version of the Bombardier CRJ-1000, will be displayed and commented on. The design changes that contributed to a change in the stability and controllability graphs were the aerodynamic improved due to the new winglet system that lead to an increase of the wing effective aspect ratio of 20%, which gives $A = 10.62$ and an increase in $C_{L_{A-h}}$ of 20% due to improvements of the high-lift devices, leading to a $C_{L_{A-h}} = 1.8$. The result of these changes can be seen more clearly in Figure 3.4. These graphs are obtained using the same methods described in section 2.5. An overview of the stability and controllability parameters of the Bombardier CRJ-EXX is given in Table 3.3. The biggest change in parameters due to the modification is a change in x_{ac} the aerodynamic centre of the aircraft, a change in the lift coefficient rates, and a change in the contribution of the flaps to the moment coefficient, which hangs together with the change in $C_{L_{A-h}}$.

Table 3.3: Stability and Controllability Parameters for the Bombardier CRJ-EXX

Stability parameters			Controllability parameters		
$\overline{x}_{ac_w}$	0.4	[-]	C_{L_h}	-0.8	[-]
$\overline{x}_{ac_{f1}}$	-0.122	[-]	$C_{m_{ac_w}}$	-0.00195	[-]
$\overline{x}_{ac_{f2}}$	0.056	[-]	$\Delta_f C_{m_{ac}}$	-0.3	[-]
$\overline{x}_{ac_n}$	-0.97	[-]	$\Delta_{fus} C_{m_{ac}}$	-0.0224	[-]
$\overline{x}_{ac}$	0.237	[-]	$\Delta_{nac} C_{m_{ac}}$	0	[-]
$C_{L\alpha_h}$	4.64	[1/rad]	$C_{m_{ac}}$	-0.324	[-]
$C_{L\alpha_h}$	6.684	[1/rad]	$C_{L_{A-h}}$	1.8	[-]
$C_{L\alpha_{A-h}}$	6.858	[1/rad]	$\overline{x}_{ac}$	0.13	[-]
$\frac{d\epsilon}{d\alpha}$	0	[-]			
$(\frac{V_h}{V})^2$	1	[-]			

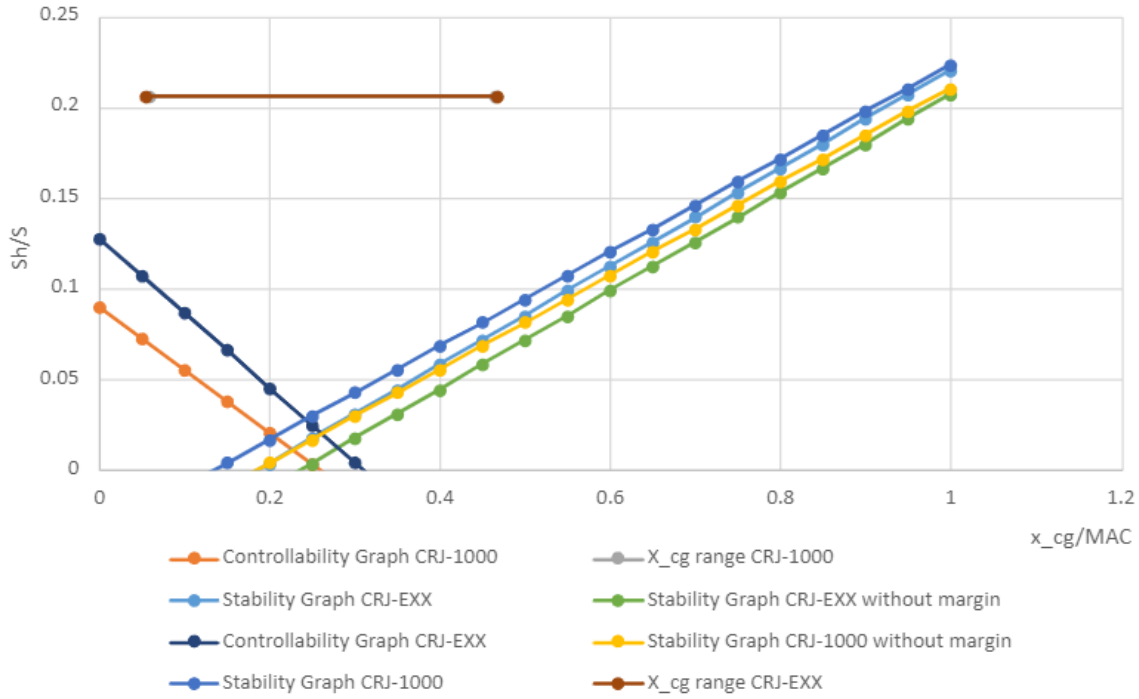

Figure 3.4: Scissor Plot for both the CRJ-1000 and CRJ-EXX

3.5 Customer Questions on the Modified Design

Phoenix works provided a set of questions in order to evaluate and discuss the modified design of the Bombardier CRJ-1000. The set of questions will be provided first after they will be addressed and answered one by one.

1. How do the aforementioned design modifications affect both longitudinal stability and controllability?
2. Would it be still possible to fulfill the longitudinal S&C requirements without changing the current horizontal tail size, longitudinal wing position and stability margin?

If NOT:

1. What would be the critical longitudinal requirement? Stability or controllability?
2. How much larger should the horizontal tail be to fulfil again both the longitudinal S&C constraints, while maintaining the same longitudinal position of the wing?
3. What design iterations (if any) would be necessary to confirm your answer?

If YES:

1. How much smaller can the horizontal tail be, while still fulfilling both the longitudinal S&C constraints and without modifying the longitudinal position of the wing neither the stability margin?
2. In this case what would become the critical longitudinal requirement? Stability or control?
3. What design iterations (if any) would be necessary to confirm your answer?
4. How do the aforementioned design modifications affect the design of the landing gears according to ground operations?

3.6 Evaluation of the Bombardier CRJ-EXX

From the scissor plot presented in section 3.4, it is clear that the design modifications made on the Bombardier CRJ-1000 lead to a change in both the stability and controllability graphs. The shift of the stability graph to the right would lead to an improvement in the stability requirements. However, looking at the controllability a compromise will have to be made. This is due to a shift to the right of controllability graph and a slight change in the slope. From this it is clear that the modifications lead to stricter requirements on the controllability for the new Bombardier CRJ-EXX, while the stability requirement becomes slightly less strict. Now, looking at the centre of gravity range for the modified design the current horizontal tail size is still inside the margins to ensure both stability and controllability of the Bombardier CRJ-EXX.

Despite the changes on the stability and controllability, it is clear that the aircraft fulfills the S&C requirements in its current configuration. Even more, there is quite a margin between the current centre of gravity range and the limits dictated by both the stability and controllability of the aircraft. More specifically, based off the scissor plot, the current centre of gravity range line can be shifted downwards until its ends meet either the stability or the controllability requirements. This leads to a decrease of the surface area of the horizontal stabilizer until $Sh/S = 0.105$. However, since the CRJ-EXX has a T-tail a margin of 15% should be taken into account to account for the deep stall risk, which leads to an actual value for Sh/S of 0.120 [8].

It is then clear that the critical requirement is the control requirement. If it is relaxed then the S_h/S ratio can be decreased even further, further optimizing the design of the aircraft. This is quite important, as the smaller

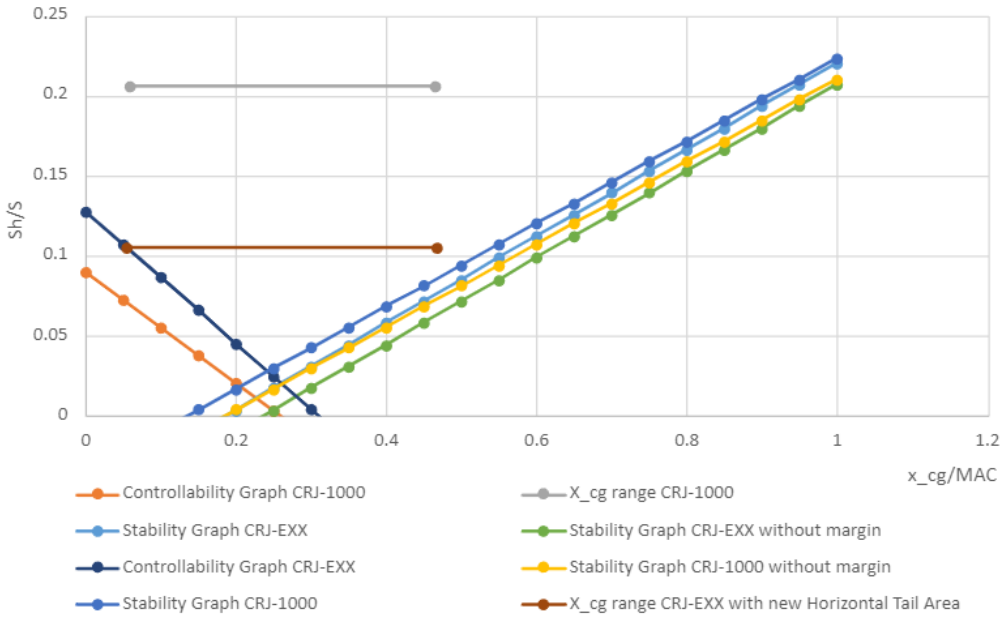

Figure 3.5: Combined Scissor Plot for CRJ-EXX with new Tail Surface

the horizontal stabilizer is, the greater the overall drag of the aircraft is during the cruise phase, which is one of the most relevant design parameters for the commercial jet aircraft.

A great care should be taken if the decision to decrease the horizontal stabilizer is taken. First of all, the plots provided above are based off the current configuration. Decreasing the horizontal stabilizer area would likely decrease the size and weight of the tailplane and shift the centre of gravity of the whole aircraft as a consequence. It is therefore not reasonable to assume that all the other lines will stay in the same place, and it is hard to predict the effect of shift of c.g. on the stability and controllability requirements.

Two steps can be taken in order to investigate the design optimization further. Firstly, a sensitivity study can be performed where the horizontal stabilizer area is decreased by a moderate amount, say 10%, and then the whole design process is repeated again in order to investigate the effect on the S&C characteristics. This would provide useful insight into how the aircraft responds to small changes in design. Alternatively, if the above mentioned process is automized sufficiently, it might be worth performing a convergence study, where the updated S&C graph is used for a new optimized S_h/S ratio which is then input to create a next generation S&C graph, until the design is converged and changes are minimal. This is significantly more complicated and is not guaranteed to be successful, since the design iteration can also diverge. However this can significantly increase the aircraft performance is the stability and controllability requirements are fulfilled with a smaller tailplane without changing the rest of the aircraft.

Finally, the effect of the design modification on the landing gears need to be discussed. First, since the position of the main wing is shifted by $50cm$ forward with respect to its old position, it is important to check if the static equilibrium requirement of the aircraft is still fulfilled. Furthermore, this will lead to a higher load distribution on the nose landing gear, which will affect the design of the nose wheel strust structure in terms of strength and stiffness, as well as the front wheel size and pressure. The second modification that has effects on the landing gear design is the change in landing gear length of $30cm$.. The change of c.g. and landing gear length means that a design iteration should be performed to check the performance of the aircraft during take-off and landing. For example, longer and more slender landing gear would likely experience higher stresses, especially during landing. This means that the landing gear, including both the wheels and the support struts, need to be redesigned in order to cope with the new loading.

References

[1] *Airport manual crj-1000*, online. [Online]. Available: https://customer.aero.bombardier.com/webd/BAG/CustSite/BRAD/RACSDocument.nsf/51aae8b2b3bfdf6685256c300045ff31/ec63f8639ff3ab9d85257c1500635bd8/$FILE/ATT82VLY.pdf/CRJ1000APMR8.pdf.

[2] MarcoDesmo27. "Excel per calcolare il peso e centraggio per crj 550-700-900-1000." (Jan. 2022), [Online]. Available: https://flightsim.to/file/26072/crj-550-700-900-1000-weight-balance-excel-calculator.

[3] Bombardier. "Crj series brochure." (2017), [Online]. Available: https://web.archive.org/web/20210828020119/https://commercialaircraft.bombardier.com/themes/bca/pdf/Bombardier_CRJ_Series_Brochure.pdf.

[4] Z. Berdowski, "Survey on standard weights of passengers and baggage," EASA, Tech. Rep., 2009.

[5] S. Suranto Putro, "An analysis on aerodynamics performance simulation of naca 23018 airfoil wings on cant angles," *Journal of Energy, Mechanical, Material and Manufacturing Engineering*, vol. 2, p. 31, Nov. 2017. DOI: 10.22219/jemmme.v2i1.4905.

[6] "Naca 23018." (Mar. 2022), [Online]. Available: http://airfoiltools.com/airfoil/details?airfoil=naca23018-il.

[7] E. Torenbeek, *Synthesis of Subsonic Airplane Design*. Dordrecht, The Netherlands: Delft University Press, 1982.

[8] D. F. Oliviero, *Ae3211-i lecture slides*, online, May 2022.

Overview Data A

Table A.1

	CRJ-1000	CRJ-EXX	
Cruise Speed	0.82	0.82	[M]
Approach Speed	0.33	0.33	[M]
(V_h/V)	1	1	[-]
$dC_{L\alpha_h}$ cruise	4.640	4.640	[1/rad]
$dC_{L\alpha_w}$ cruise	6.359	6.684	[1/rad]
$dC_{L\alpha_{A-h}}$ cruise	6.532	6.858	[1/rad]
$\frac{d\epsilon}{d\alpha}$	0	0	[-]
$\overline{x}_{ac_w}$ cruise	0.36	0.4	[-]
$\overline{x}_{ac_{f1}}$ cruise	-0.128	-0.122	[-]
$\overline{x}_{ac_{f2}}$ cruise	0.056	0.056	[-]
$\overline{x}_{ac_n}$ cruise	-0.102	-0.97	[-]
$\overline{x}_{ac}$ cruise	0.186	0.237	[-]
$\overline{x}_{ac_w}$ approach	0.36	0.37	[-]
$\overline{x}_{ac_{f1}}$ approach	-0.17	-0.165	[-]
$\overline{x}_{ac_{f2}}$ approach	-0.056	0.056	[-]
$\overline{x}_{ac_n}$ approach	-0.136	-0.132	[-]
$\overline{x}_{ac}$ approach	0.11	0.13	[-]
C_{l_h}	-0.8	-0.8	[-]
$C_{m0_{airfoil}}$	-0.00189	-0.00195	[-]
$\Delta_{fus}C_{m_{ac}}$	-0.0235	-0.0224	[-]
$\Delta_f C_{m_{ac}}$	-0.2	-0.3	[-]
$\Delta_{nac}C_{m_{ac}}$	0	0	[-]
$C_{m_{ac}}$	-0.225	-0.324	[-]

Aircraft Dimensional Parameter Determination

B

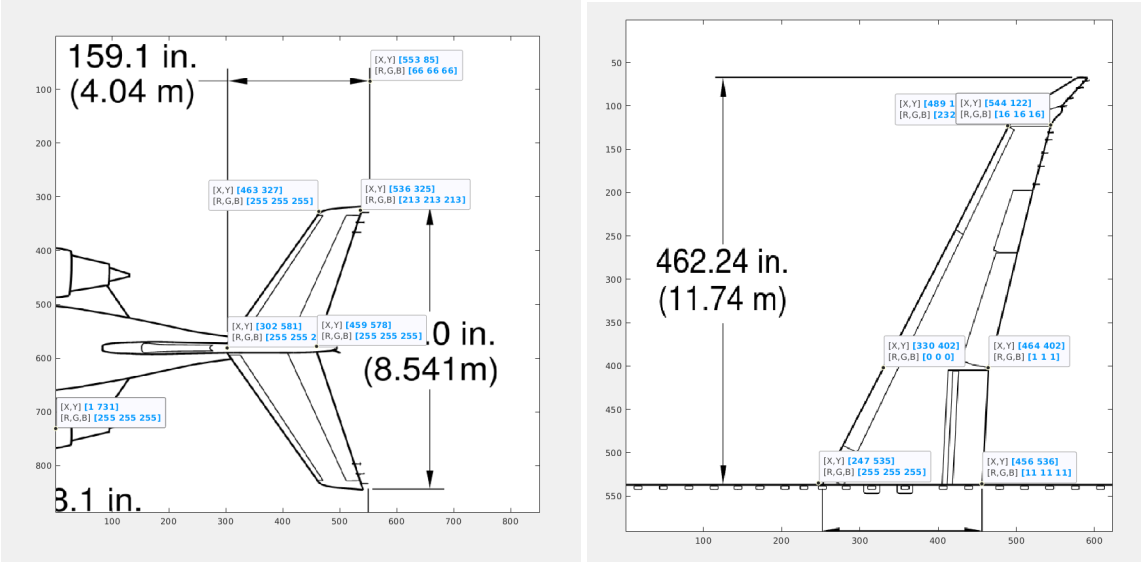

(a) Top view of the empennage.

(b) Top view of the main wing.

Figure B.1: Top View of wing and horizontal tail

Organization C

Since a group can only operate in an efficient way, if it is organized well, a short discussion of the organization for this report will be presented below.

The group work of this report was divided across the member based on who was the most confident in their knowledge of the relevant topic. For the calculation of centre of gravity and scissor plots, the group worked together since a good understanding of other deliverables is needed, even though one member was assigned responsible. This also applies to all the other deliverables in lesser extent. This way, work of people was constantly checked by other members of the group in order to avoid large mistake which could jeopardize the report. Still, the writing of the report sections was left to the people who were involved the most in a certain task in order to make sure that the quality of writing is highest.

Furthermore, the group decided to work on campus during the majority of the work to improve the group efficiency, since working online leads to a lack of communication. However, when an online session was planned discord was used as the communication source. Moreover, some discussions and progress was communicated using WhatsApp. Finally, all the graphs and data used in this report was collected in a shared google drive, so that everyone of the group could access the neccessary data at any point in time.

Table C.1 presents the task distribution of the various deliverables of the assignment.

Table C.1: Task distribution

Member	Task
Alex Krochak (5015529)	CRJ-1000 Data research
	CRJ-EXX Customer questions
Julie Paddeu (4997522)	CRJ-1000 Data Research
	CRJ-1000 Scissor plots
	CRJ-EXX Scissor plots
João Rodríguez (4993578)	CRJ-EXX c.g. determination
	CRJ-EXX Weights determination
Oliver Ross (5008042)	Geometry parameters determination
Lorenz Veithen (5075211)	Aerodynamic parameters determination
	Stability parameters determination
Niek Zandvliet (4796403)	CRJ-1000 c.g. determination
	CRJ-1000 Weights determination

Table C.2 presents the task distribution of the various sections of the report.

Table C.2: Report distribution

Section	Member
1. Introduction	Oliver Ross
2.1 C.G. Parameters	Alex Krochak
	Niek Zandvliet
2.2 Aero. Parameters	Lorenz Veithen
2.3 Geom. Parameters	Oliver Ross
2.4 Loading Diagram	Niek Zandvliet
2.5 Scissor Plot	Julie Paddeu
	Lorenz Veithen
3.1 CRJ-EXX	Julie Paddeu
3.2 Modified Weights	Joao Rodriguez
3.3 Modified C.G.	Joao Rodriguez
3.4 Modiffied Scissor Plot	Julie Paddeu
3.5 Customer Questions	Oliver Ross
3.6 Evaluation Design	Alex Krochak
	Julie Paddeu